Michigan State University
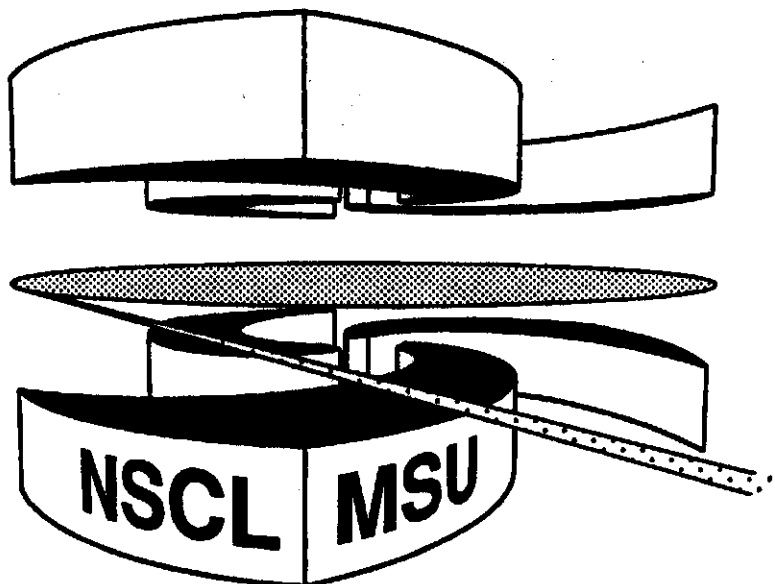
National Superconducting Cyclotron Laboratory

TEMPERATURE DEPENDENCE OF THE GIANT DIPOLE RESONANCE WIDTH IN ^{208}Pb

E. RAMAKRISHNAN, A. AZHARI, J.R. BEENE, R.J. CHARITY,
M.L. HALBERT, P.-F. HUA, R.A. KRYGER, P.E. MUELLER,
R. PFAFF, D.G. SARANTITES, L.G. SOBOTKA,
M. THOENNESSEN, G. VAN BUREN, R.L. VARNER,
S. YOKOYAMA

Temperature Dependence of the Giant Dipole Resonance Width in ^{208}Pb

E. Ramakrishnan [a,1], A. Azhari [a], J. R. Beene [b], R. J. Charity [c],
M. L. Halbert [b], P.-F. Hua [c], R. A. Kryger [a], P. E. Mueller [b],
R. Pfaff [a], D. G. Sarantites [c], L. G. Sobotka [c], M. Thoennessen [a],
G. Van Buren [c], R. L. Varner [b], S. Yokoyama"

[a] *National Superconducting Cyclotron Laboratory,*
and Department of Physics & Astronomy,
Michigan *State University, East Lansing, MI 48824, USA*

[b] *Oak Ridge National Labomtory, Oak Ridge, TN 37831, USA*

[c] *Department of Chemistry, Washington University, St. Louis, MO 63130, USA*

The evolution of the giant dipole resonance (GDR) in hot ^{208}Pb nuclei was studied by measuring high energy y-rays from the decay of the resonance built on excited states. Nuclei in the excitation energy range of 40-110 MeV were populated by inelastic scattering of 40 MeV/nucleon o-particles. The GDR width was observed to increase systematically from 4 MeV at the ground state to ~8 MeV at the highest excitation energy.

The excitation energy dependence of the giant dipole resonance (GDR) width is still one of the open questions in the description of collective modes in nuclei at finite temperatures [1,2]. The increase of the GDR width with increasing excitation energy has been explained for example by the coupling of the resonance to shape variations of the nucleus induced by temperature and angular momentum [3], or by convolution of Landau damping (one-body) with the damping due to two-body collisions [4]. Experimentally, the evolution of the GDR as a function of temperature is studied by the decay of highly excited

---

[1] Present address: Cyclotron Institute, Texas A&M University, College Station, Texas 77843, USA. E-mail address: ramak@comp.tamu.edu

compound nuclei formed in fusion evaporation reactions [5]. In these measurements it is difficult to disentangle the temperature dependence of the width from the influence of the increasing angular momentum [6].

Recently, we have developed a different method to populate these highly excited compound systems [7]. Light ion inelastic scattering was used to populate low angular momentum states in the target nucleus up to fairly high excitation energies. The energy loss of the projectile can be related to excitation energy of the target and thus, by selecting narrow ranges of the energy loss, the evolution of the GDR can be studied as a function of the initial excitation energy of the system. This method probes the temperature dependence of the GDR at low angular momenta, and is complementary to the fusion measurements which select predominantly high angular momenta by gating on the γ-ray multiplicity [6], and to the method of difference spectra which selects compound nuclei from a restricted range of angular momentum and temperature [8].

Most studies of the intrinsic width of the GDR as a function of temperature have concentrated on Sn isotopes [6] because these nuclei maintain a spherical shape and therefore a single component GDR even at high excitation energies. In this letter we present a study of the temperature dependence of the GDR width in excited ^{208}Pb nuclei. ^{208}Pb is also spherical but in contrast to Sn it exhibits very strong shell effects. The evolution of the GDR width should contain information about the vanishing of the shell effects at finite temperature, which is predicted to occur at a temperature of ~1.5 MeV [9].

We populated highly excited states in ^{208}Pb by inelastic scattering of α-particles. The experiment was performed at the National Superconducting Cyclotron Laboratory (NSCL). A 3 mg/cm^2 target was bombarded by a 40 MeV/nucleon beam of α-particles extracted from the K1200 cyclotron. The *Dwarf Ball/Wall 4π CsI(Tl)* array [10] was utilized to measure the inelastically scattered projectile nuclei and other light charged reaction products. The Wall array consisted of 35 close-packed detectors arranged in four rings centered at laboratory angles of 14.78°, 22.39°, 23.18° and 31.03° and covering the angular range of ~10° to ~36°. The Ball array consisted of 64 close-packed detectors covering laboratory angles of ~36° to ~155°. The detectors of the Wall array were calibrated by measuring the elastic scattering peak for α-particles at various beam energies. High energy γ rays from the decay of the GDR in the target were measured in coincidence with particles in the Wall array. The γ rays were measured using 95 BaF$_2$ detectors arranged in 5 close-packed arrays of 19 detectors each. The five arrays were placed at a distance of ~40 cm from the target, at laboratory angles of 60°(2), 72°(2) and 112°(1). The solid angle coverage of the BaF$_2$ arrays amounted to ~17% of 4π. Separation between γ rays and neutrons in the detectors was achieved by time of flight measurement. The detectors were calibrated at low energies using radioactive sources,
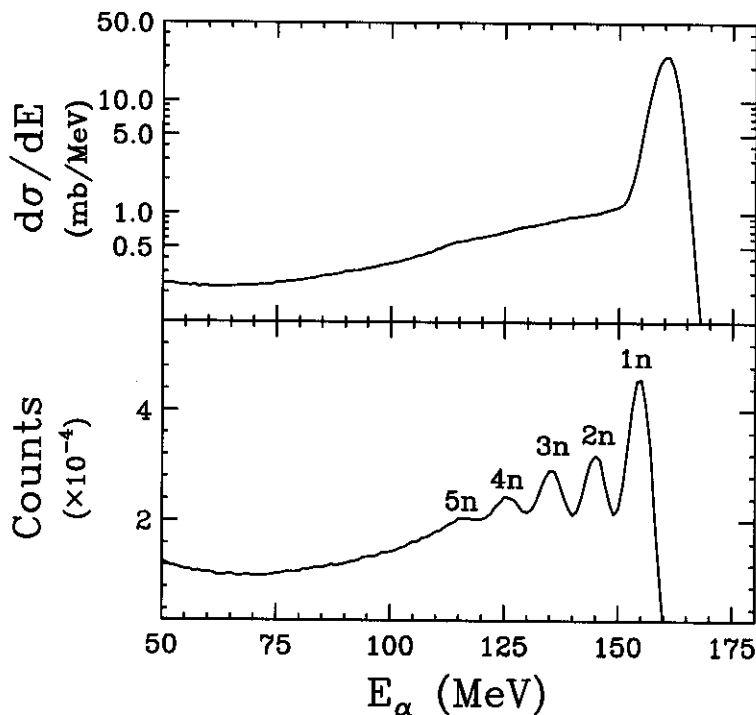
2

Fig. 1. α-particle spectra at 15° in laboratory. The top panel displays the singles spectrum and the bottom panel displays the spectrum in coincidence with γ-rays of energy $E_\gamma \geq 4$MeV.

and at an intermediate energy by measuring the ground state γ-ray decay of the 15.11 MeV state in ^{12}C excited by inelastic α-particle scattering. The measured energy loss of cosmic-ray muons in the detector volume provided an additional calibration point at an energy of $\sim$40 MeV. The response of the detector geometry to γ-rays was simulated using the code GEANT3 [11].

In order to correlate the energy loss of the α-particles with the excitation energy of the target nucleus, two conditions have to be fulfilled: (i) the scattered particle has to excite the target as a whole and not interact with individual nucleons or clusters resulting in knock-out or pickup-decay reactions and (ii) the highly excited target should not decay by pre-equilibrium emission of particles but instead should equilibrate rapidly to form a compound nuclear state. It has been shown in an inelastic scattering measurement of ^{17}O on ^{208}Pb that a coincidence measurement of the scattered particle with γ rays is sensitive to both of the above conditions [12]. The particle spectrum in coincidence with γ rays ($E_\gamma \geq 1$ MeV) exhibited structures up to $\sim$45 MeV which could be interpreted as the successive opening of neutron evaporation channels in the decay of the excited target nucleus. These structures should be present only if all the energy lost by the projectile is converted to excitation energy in the equilibrated target system.

Figure 1 displays a similar plot for the present experiment. The top panel

shows the singles spectrum of the scattered α-particles measured in the most forward ring of the Wall array. In addition to the elastic scattering peak at the incident beam energy it shows a broad featureless continuum at higher projectile energy losses. The bottom panel shows the α-particle spectrum in coincidence with γ-rays with $E_\gamma \geq 4$ MeV. Structures according to the indicated neutron evaporation thresholds can be seen up to an excitation energy of $\sim$50 MeV. At excitation energies above 50 MeV higher thresholds are washed out and cannot be observed anymore.

In addition to target excitation other reaction mechanisms like single nucleon knock-out or pickup-decay processes cannot be ruled out [13]. Contributions from such background processes were estimated by analysing events where protons were detected in the Dwarf Ball/Wall array in coincidence with α-particles in the Dwarf Wall array. Such events were found to be predominantly localized at the kinematic limit where the total energy is shared by the proton and the α-particle, leaving the target nucleus in the ground state or low-lying excited states [14]. Contributions to the coincident γ-ray spectrum in the GDR range from these background processes is therefore negligible.

At α-particle energies below $\sim$50 MeV the inelastic cross section begins to rise due to contributions from pre-equilibrium processes where the incoming α-particle interacts with target nucleons resulting in the emission of one or more secondary α-particles [15]. The present analysis was therefore restricted to α-particle energies above 50 MeV. In the following the energy-loss of the α particles is assumed to be directly correlated to the excitation energy of an equilibrated compound nucleus. The decay of the compound nucleus can then be treated within a statistical model and extracted γ-ray spectra should exhibit the typical GDR enhancement.

The presence of this enhancement in the data is shown in Figure 2 for two target excitation energy ranges. The upper panels display the γ-ray spectra ($\bullet$) for the excitation energy ranges of 60–70 MeV (a) and 100–110 MeV (b), in coincidence with α-particles of energies 90–100 MeV and 50–60 MeV, respectively. The characteristic GDR bump is located around 13 MeV, corresponding to the GDR energy in ^{208}Pb. A comparison between the spectra reveals additional evidence for the dominance of target excitation up to large α-particle energy losses. The emission probability for a GDR γ-ray increases with increasing excitation energy of the compound nucleus [16]. Thus, if a larger energy-loss of the α particles corresponds to higher target excitation energy, the GDR γ-ray yield should increase with energy-loss. This effect is indeed observed. The γ-ray yield in the region of the GDR (10–15 MeV) relative to the statistical γ rays (5–8 MeV) is bigger for the larger α energy-loss ($E_\alpha = 50$–60 MeV, (b)) compared to the smaller energy loss ($E_\alpha = 90$–100 MeV, (a)).

The γ-ray spectra were fitted with calculations performed within the standard

4

statistical model using a modified version of the evaporation code CASCADE [17]. The initial population of the compound nucleus for each excitation energy bin was obtained from the spectra of inelastically scattered α particles from the Wall array by converting the energy loss to excitation energy. The excitation energy range was divided in 10 MeV-wide bins and the counts in the singles spectra for each bin was taken to be the initial population of the excited compound nucleus. These counts were distributed over a range of calculated angular momenta [7]. The angular momentum range was estimated from the linear momentum transferred to the target obtained from the energy loss of the projectile and with the assumption that the impact parameters contributing to the inelastic scattering are concentrated in the nuclear surface. The impact parameter was allowed to vary in the range of the 'nuclear interaction radius' to the sum of the 'matter half-density radii' of the target and projectile nuclei [18].

In addition to the initial compound nucleus distribution the level density description for the subsequent decay had to be modified. At low excitation energies, the closed shell structure of ^{208}Pb has a strong influence on the level density [19]. The standard linear interpolation method between the level densities at low and high excitation energies used in CASCADE did not yield a smooth increase of the level densities with increasing excitation energy. Due to the strong shell effects in ^{208}Pb at low excitation energies, the differences between the level density parameter a at low excitation energies ($a \sim A/30$) [9] and at high excitation energies ($a \sim A/10$) are too large. Thus, the Reisdorf level density parameterization [20] was incorporated in the code [14].

The exponential tail at high γ-ray energies due to bremsstrahlung processes were fitted between 25–30 MeV with an exponential $\exp(-E_\gamma/E_0)$ and the slope parameter was chosen to be $E_0 = 13 \pm 1$ MeV from systematics [21,22]. The calculated non-statistical contribution was added to the statistical calculations after folding both contributions with the detector response. The sum rule strength extracted from fits to the data decreased from $\sim$100% to $\sim$60% with increasing excitation energy. This apparent decrease indicates a larger contribution of low energy γ-rays (< 8 MeV) which could be attributed to the increasing importance of the background processes discussed earlier and that did not induce collective excitation in the target but nevertheless resulted in the emission of γ-rays below $\sim$8 MeV. This increase of low energy γ-rays did not influence the extraction of the GDR width. The final results of the statistical calculations are included (solid line) in the upper panels of figure 2. The calculations were normalized to the data in the low energy region of 7–8 MeV and the normalization factors varied from $\sim$0.8 to $\sim$1.0. The lower panels of figure 2 display the measured spectra and the calculations on a linear scale for target excitation energies of 60–70 MeV (c) and 100–110 MeV (d) in order to show the quality of the fits. The linear plots were obtained by dividing the measured spectra as well as the calculations by a second statistical calcula-
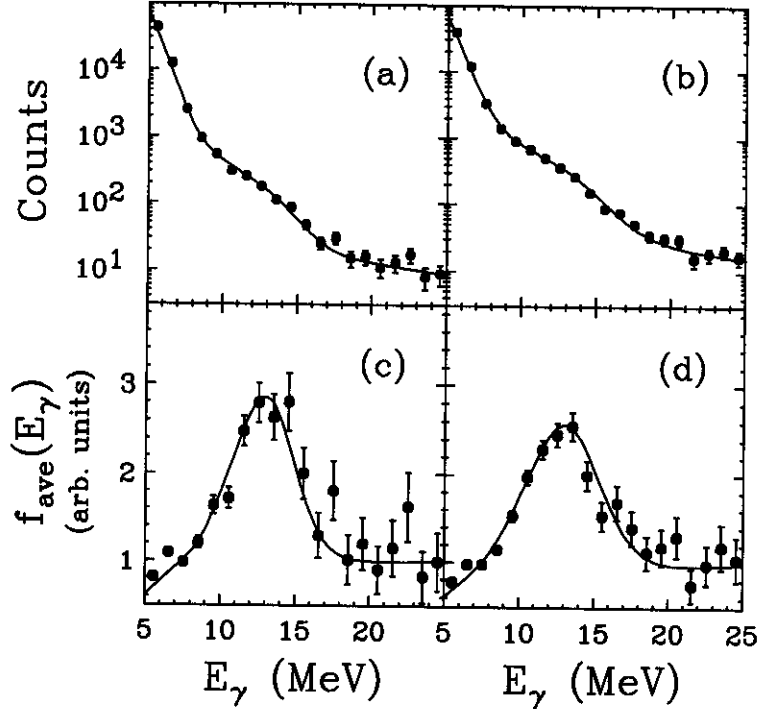
Fig. 2. Coincidence γ-ray spectra from two excitation energy cuts. The upper two panels display the spectra (●) for excitation energies of 60–70 MeV (a) and 100–110 MeV (b). The bottom panels display the same spectra on a linear scale obtained as explained in text. The solid lines are results of statistical model calculations.

tion with an $E1$ strength function with a strength of 0.2 Weisskopf units. The increase of the GDR width at the larger excitation energy (d) is apparent.

The GDR width extracted from these calculations was observed to increase systematically over the excitation energy range of 40 to 110 MeV. Figure 3 displays the resonance width as a function of nuclear temperature (●). The uncertainty of ±0.5 MeV on the extracted widths includes the statistical error and the uncertainty of the bremsstrahlung contribution, but it does not include any systematic dependence on the level density description. The target excitation energy was converted to nuclear temperature using the expression $< T > = \sqrt{E_{eff}/a(E_{eff})}$. The effective excitation energy E_{eff} was calculated by subtracting the mean rotational energy and the giant dipole resonance energy from the mean excitation energy of the input population. The quantity $a(E_{eff})$ is the energy dependent level density parameter employed in the statistical calculations. The GDR width of the ground-state (4 MeV [23]) is also included in figure 3.

The width data are consistent with a quadratic dependence on temperature and can be described by the relation $\Gamma_{GDR} = 4.0 + 0.89T^2$ shown as the solid curve in the top panel of Figure 3. A T^2 dependence is expected from two body collisional damping [24], however the observed dependence is much stronger
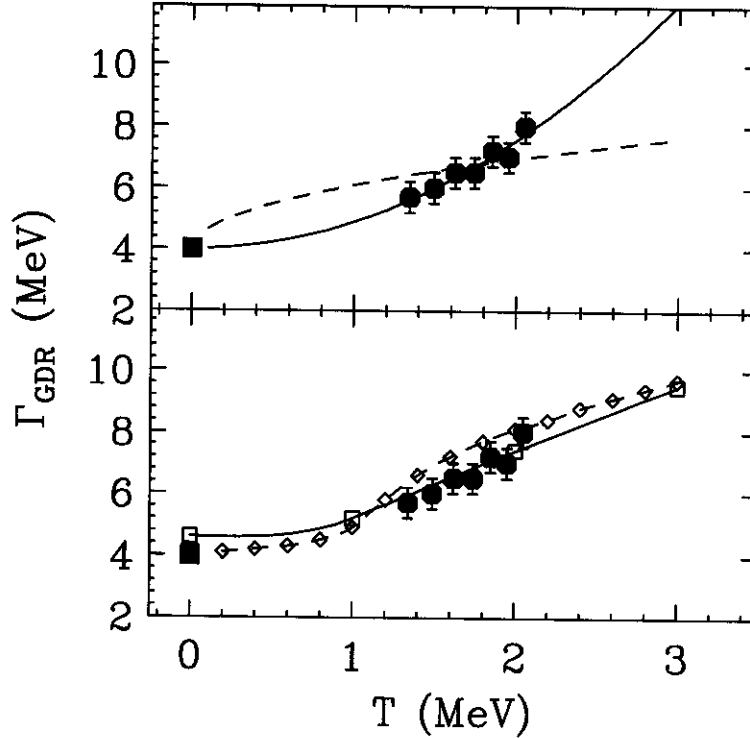
Fig. 3. The resonance width obtained from fits to the γ-ray spectra as a function of excitation energy (filled circles). The ground state width (filled square) is also shown. The upper panel includes fits with a $\sqrt{T}$ dependence (dashed) and a T^2 dependence (solid) and the lower panel compares the data with an adiabatic coupling calculation (dashed) and a collisional damping calculation (solid).

than that predicted by the most recent calculations [4]. In contrast, according to adiabatic calculations the increase of the GDR width with temperature is due to the thermal averaging over different nuclear shapes, leading to a $\sqrt{T}$ dependence [25]. The fit $\Gamma_{GDR} = 4.0 + 2.1\sqrt{T}$ shown as the dashed line in the top panel of figure 3 clearly does not describe the data. The latter calculations, however do describe the recent inelastic scattering data in ^{120}Sn [7,26]. One difference between ^{120}Sn and ^{208}Pb is the strong shell effects present in the latter case. Ormand et al. have performed the adiabatic coupling calculations for ^{208}Pb which include shell effects calculated by the Nilsson-Strutinsky method extended to finite temperatures [26]. The results of these calculations are shown as the solid line and open diamonds in the bottom panel of figure 3. The calculation still exhibits the $\sqrt{T}$ dependence, however, the onset of this behavior is delayed because of the strong influence of the shell effects at low temperatures. The shell effects begin to wash out around 1 MeV. Although the calculation slightly overpredicts the data it reproduces the trend fairly well.

The dashed line and the open squares in the bottom panel of figure 3 show a recent calculation based on the linearized Vlasov equation which includes the interplay between the collisional (two-body) damping and the Landau

7

(one-body) damping [4,27]. The combination of both damping effects leads to a stronger T^2 effect than given by two-body damping alone. Although the ground state width is overpredicted the calculations reproduce the data well.

It should be mentioned that direct comparison of these calculations with the data is not straight forward. The determination of the temperature depends critically on the level density parameter. In order to get a more quantitative description of the data, it is necessary to incorporate the calculated GDR strength function in the statistical model code and compare the experimental spectra directly and not just the extracted GDR width. These calculations are currently in progress and will perhaps be able to distinguish between the two descriptions of the broadening of the GDR as a function of temperature.

It would be desirable to extend the present measurements to lower as well as to higher temperatures in order to distinguish between the two theoretical approaches. However, temperatures below ~1.3 MeV (corresponding to excitation energies of ~40 MeV) are not accessible by GDR γ-ray decay studies because the probability of emitting a 15 MeV γ-ray at these energies is extremely small and thus the GDR contribution to the spectra is too small to extract the GDR width. Temperatures higher than 2 MeV should be accessible by using heavy-ion scattering which should not be limited by pre-equilibrium emission at large energy losses.

The present measurement has demonstrated the feasibility of studying the evolution of nuclear shapes in stable nuclei using light ion inelastic scattering. Low angular momentum states are populated in the scattering process. The shape evolution can thus be studied as a function of temperature, decoupled from spin effects. In this measurement, the width of the GDR in hot ^{208}Pb nuclei was observed to increase systematically with excitation energy. This increase is consistent with a $\sqrt{T}$ behavior of the adiabatic model after the strong shell effects of ^{208}Pb have been taken into account as well as with a T^2 dependence of the collisional damping model after the interplay with the Landau damping was included.

References

[1] Ph. Chomaz, Phys. Lett. **B 347**, 1 (1995), and references therein.

[2] "Proceedings of the Groningen Conference on Giant Resonances", 28. June - 1. July 1995, Nucl. Phys. **A599** (1996).

[3] M. Gallardo *et al.*, Nucl. Phys. **A443**, 415 (1985). Y. Alhassid, B. Bush, and S. Levit, Phys. Rev. Lett. **61**, 294 (1988). J. M. Pacheco, C. Yannouleas, and R. A. Broglia, Phys. Rev. Lett. **61**, 1926 (1988). Y. Alhassid and B. Bush, Nucl. Phys. **A509**, 461 (1990).

[4] V. Baran, M. Colonna, M. DiToro, A. Guarnera, V.N. Kondratyev, and A. Smerzi, Nucl. Phys. **A599**, 29c (1996).

[5] J. J. Gaardhøje, Ann. Rev. Nucl. Part. Sci. **42**, 483 (1992).

[6] A. Bracco, F. Camera, M. Mattiuzzi, B. Million, M. Pignanelli, J.J. Gaardhoje, A. Maj, T. Ramsoy, T. Tveter, and Z. Zelazny, Phys. Rev. Lett. **74**, 3748 (1995) and references therein.

[7] E. Ramakrishnan *et al.*, Phys. Rev. Lett. **76**, 2025 (1996).

[8] J. P. S. van Schagen *et al.*, Phys. Lett. **B 343**, 64 (1995).

[9] A. Bohr and B. R. Mottelson *"Nuclear Structure"*, Volume II, p. 611, (W. A. Benjamin, Inc., Reading, MA, 1975).

[10] D. W. Stracener *et al.*, Nucl. Instr. and Meth. A **294**, 485 (1990).

[11] R. Brun *et al.*, GEANT3 Users Guide, Data Handling Division DD/EE/84-1, CERN 1986.

[12] M. Thoennessen *et al.*, Phys. Rev. C **43**, R12 (1991).

[13] G. Chenevert *et al.*, Phys. Rev. Lett **27**, 434 (1971). H. G. Bohlen *et al.*, Z. Phys. A **320**, 237 (1985). D. Hilscher *et al.*, Phys. Rev. C **20**, 556 (1979). Y. Blumenfeld *et al.*, Nucl. Phys. **A445**,151 (1985). F. E. Bertrand *et al.*, Phys. Rev. C **35**, 111 (1987).

[14] E. Ramakrishnan, Ph.D. thesis, Michigan State University, unpublished (1995).

[15] M. Chadwick *et al.*, submitted to Heavy Ion Physics (1996).

[16] K. A. Snover Ann. Rev. Nucl. Part. Sci. **36**, 545 (1986).

[17] F. Pühlhofer, Nucl. Phys. **A280**, 267 (1977).

[18] W. W. Wilcke *et al.*, Atomic and Nuclear Data Tables **25**, 389 (1980).

[19] W. Dilg *et al.*, Nucl. Phys. **A217** 269 (1973).

[20] W. Reisdorf, Z. Phys. A **300**, 227 (1981).

[21] H. Nifenecker & J. A. Pinston, Ann. Rev. Nuc. Part. Sci., **40**, 113 (1990).

[22] V. Metag, Ann. Phys. (Leipzig) **48** 121 (1991), and references therein.

[23] S. S. Dietrich and B. L. Berman, At. Data Nucl. Data Tables, **38**, 199 (1988).

[24] A. Smerzi, A. Bonasera, and M. DiToro, Phys. Rev. C **44**, 1713 (1991).

[25] R. A. Broglia, P. F. Bortignon, and A. Bracco, Prog. Part. Nucl. Phys. **28**, 517 (1992).

[26] W. E. Ormand, P. F. Bortignon, and R. A. Broglia, submitted to Phys. Rev. Lett. (1996).

[27] M. DiToro, private communication.